

$\gamma N \rightarrow \Delta$ transition form factors in Quenched and $N_F = 2$ QCD*

C. Alexandrou^a, Ph. de Forcrand^b, Th. Lippert^c, H. Neff^{†d}, J. W. Negele^e, K. Schilling^e, W. Schroers^{‡e} and A. Tsapalis^{§a}

^aDepartment of Physics, University of Cyprus, CY-1678 Nicosia, Cyprus

^bETH-Zürich, CH-8093 Zürich and CERN Theory Division, CH-1211 Geneva 23, Switzerland

^cDepartment of Physics, University of Wuppertal, D-42097 Wuppertal, Germany

^dInstitute of Accelerating Systems and Applications and Department of Physics, University of Athens, Athens, Greece, and Physics Department, Boston University, Boston, Massachusetts 02215, USA

^eCenter for Theoretical Physics, Laboratory for Nuclear Science and Department of Physics, Massachusetts Institute of Technology, Cambridge, Massachusetts 02139, USA

Calculations of the magnetic dipole, electric quadrupole and Coulomb quadrupole amplitudes for the transition $\gamma N \rightarrow \Delta$ are presented both in quenched QCD and with two flavours of degenerate dynamical quarks.

1. Introduction

The shape of the proton is a fundamental issue in hadron structure that depends on QCD dynamics. The purpose of this study is to gain insight as to what the mechanism that produces the deformation is. Deformation can be determined from hadron wave functions obtained via two- and three- density gauge invariant correlators [1]. However the intrinsic quadrupole moment is not always observable and it vanishes between hadronic states of spin less than one. Therefore to determine the deformation of the proton one searches for quadrupole strength in the transition $\gamma N \rightarrow \Delta(1232)$ with real or virtual photons. Spin-parity selection rules allow a magnetic dipole, an electric quadrupole and a Coulomb quadrupole amplitude, which in the Sachs decomposition are given in terms of the form factors \mathcal{G}_{M1} , \mathcal{G}_{E2} and \mathcal{G}_{C2} that depend on the momentum transfer $q^2 = (p' - p)^2$. Deviation from zero of the ratios [2,3]

$$R_{EM} = -\frac{\mathcal{G}_{E2}}{\mathcal{G}_{M1}} \quad R_{SM} = -\frac{|\mathbf{q}|}{2m_\Delta} \frac{\mathcal{G}_{C2}}{\mathcal{G}_{M1}} \quad (1)$$

*Talk presented by A. Tsapalis

†Acknowledges funding from the European network ESOP (HPRN-CT-2000-00130) and the University of Cyprus

‡Supported by the Alexander von Humboldt Foundation

§Supported by the Levendis Foundation

indicates deformation of the nucleon and/or Δ . These ratios have been accurately measured in recent electroproduction experiments at Bates and Jefferson Labs [4] at various momentum transfers.

2. Lattice matrix elements

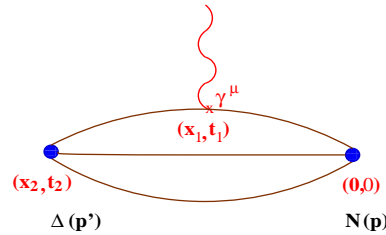


Figure 1. $\gamma N \rightarrow \Delta$ matrix element. The photon couples to a quark in the nucleon at time separation t_1 from the source to produce a Δ .

We evaluate the 3-point function, $\langle G_\sigma^{\Delta j^\mu N}(t; \mathbf{p}', \mathbf{p}; \Gamma) \rangle$ shown schematically in Fig. 1, as well as $\langle G_\sigma^{N j^\mu \Delta}(t_2, t_1; \mathbf{p}', \mathbf{p}; \Gamma) \rangle$ for the reverse $\Delta \rightarrow \gamma N$ transition. Exponential decays and normalization constants cancel in the ratio $R_\sigma(t_2, t_1; \mathbf{p}', \mathbf{p}; \Gamma; \mu) =$

$$\left[\frac{\langle G_\sigma^{\Delta j^\mu N}(t_2, t_1; \mathbf{p}', \mathbf{p}; \Gamma) \rangle \langle G_\sigma^{N j^\mu \Delta}(t_2, t_1; -\mathbf{p}, -\mathbf{p}'; \Gamma^\dagger) \rangle}{\langle \delta_{ij} G_{ij}^{\Delta \Delta}(t_2, \mathbf{p}'; \Gamma_4) \rangle \langle G^{NN}(t_2, -\mathbf{p}; \Gamma_4) \rangle} \right]^{1/2} \quad (2)$$

$t_2 - t_1 \gg 1, t_1 \gg 1$

$\Pi_\sigma(\mathbf{p}', \mathbf{p}; \Gamma; \mu),$

where G^{NN} and $G_{ij}^{\Delta\Delta}$ are the nucleon and Δ two point functions evaluated in the standard way.

The Sachs form factors are obtained by appropriate combinations of the Δ spin-index σ , current direction μ and projection matrices Γ . For instance, in the Δ rest frame $\vec{p}' = 0$, $\vec{q} = (q, 0, 0)$ [2,3] we have

$$\begin{aligned}\mathcal{G}_{M1} &= \mathcal{A} \frac{1}{|\mathbf{q}|} \Pi_2(\mathbf{0}, -\mathbf{q}; +i \Gamma_4; 3) \\ \mathcal{G}_{E2} &= \mathcal{A} \frac{1}{3|\mathbf{q}|} \left[\Pi_3(\mathbf{0}, -\mathbf{q}; \Gamma_1; 3) + \Pi_1(\mathbf{0}, -\mathbf{q}; \Gamma_3; 3) \right] \\ \mathcal{G}_{C2} &= \mathcal{A} \frac{M_\Delta}{\mathbf{q}^2} \Pi_1(\mathbf{0}, -\mathbf{q}; -i \Gamma_1; 4)\end{aligned}\quad (3)$$

where \mathcal{A} is a kinematical factor.

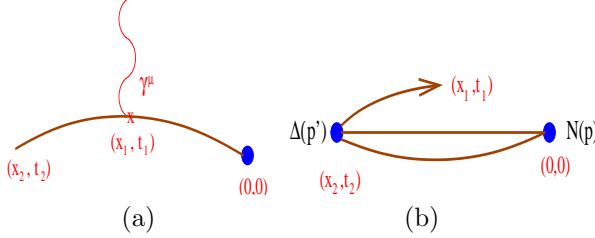


Figure 2. (a) Fixed operator and (b) fixed source sequential propagators.

We use two methods to compute the sequential propagator needed to build the 3-point function: (a) We evaluate the quark line with the photon insertion, shown schematically in Fig. 2(a) by computing the sequential propagator at fixed momentum transfer \mathbf{q} and fixed time t_1 . We look for a plateau by varying the sink-source separation time t_2 . The final and initial states can be chosen at the end. (b) We evaluate the backward sequential propagator shown schematically in Fig. 2(b) by fixing the initial and final states. t_2 is fixed and a plateau is searched for by varying t_1 . Since the momentum transfer is specified only at the end the $\gamma N \rightarrow \Delta$ form factors can be evaluated at all lattice momenta.

3. Results

Using the fixed operator method for the sequential propagator we obtain, for the same value of \mathbf{q} , two kinematically different cases: one with the Δ at rest and the other with the nucleon at

Table 1

Q^2 (GeV ²)	κ	m_π/m_ρ	Number of confs
Quenched $\beta = 6.0$ $16^3 \times 32$ $\mathbf{q}^2 = 0.64$ GeV ²			
0.64	0.1530	0.84	100
0.64	0.1540	0.78	100
0.64	0.1550	0.70	100
Quenched $\beta = 6.0$ $32^3 \times 64$ $\mathbf{q}^2 = 0.64$ GeV ²			
0.64	0.1550	0.69	100
Unquenched $\beta = 5.6$ $16^3 \times 32$ [5] $\mathbf{q}^2 = 0.54$ GeV ²			
0.54	0.1560	0.83	196
0.54	0.1565	0.81	200
0.54	0.1570	0.76	201
0.54	0.1575	0.68	200

rest. The parameters of our lattices are given in Table 1 where we used the nucleon mass in the chiral limit to convert to physical units, and $Q^2 = -q^2$ is evaluated in the rest frame of the Δ .

We check for finite volume effects by comparing results in the quenched theory on lattices of size $16^3 \times 32$ and $32^3 \times 64$ at the same momentum transfer at $\kappa = 0.1550$. Assuming a $1/\text{volume}$ dependence we find that on the small volumes there is a (10 – 15)% correction as compared to the infinite volume result whereas on the large lattice the volume correction is negligible. In Fig. 3 we show quenched and unquenched results for \mathcal{G}_{M1} and \mathcal{G}_{E2} at the same momentum transfer and similar ratios of pion to rho mass. Unquenching leads to a stronger mass dependence but leaves the ratio R_{EM} largely unaffected, giving values in the range of $-(2 - 4)\%$. The fact that no increase of R_{EM} is observed means that pion contributions to this ratio are small for these heavy pions. In Fig. 3 we also show results for \mathcal{G}_{C2} with Δ static for the large quenched lattice for which we obtain the best signal. Although \mathcal{G}_{C2} is within one standard deviation of zero, it is positive at all κ -values giving a negative R_{SM} in agreement with experiment.

Using the fixed sink method for the sequential propagator we show in Fig. 4 preliminary results for the q^2 -dependence of \mathcal{G}_{M1} obtained using 50 quenched configurations at $\kappa = 0.1554$ together with a fit to the preferred phenomenolog-

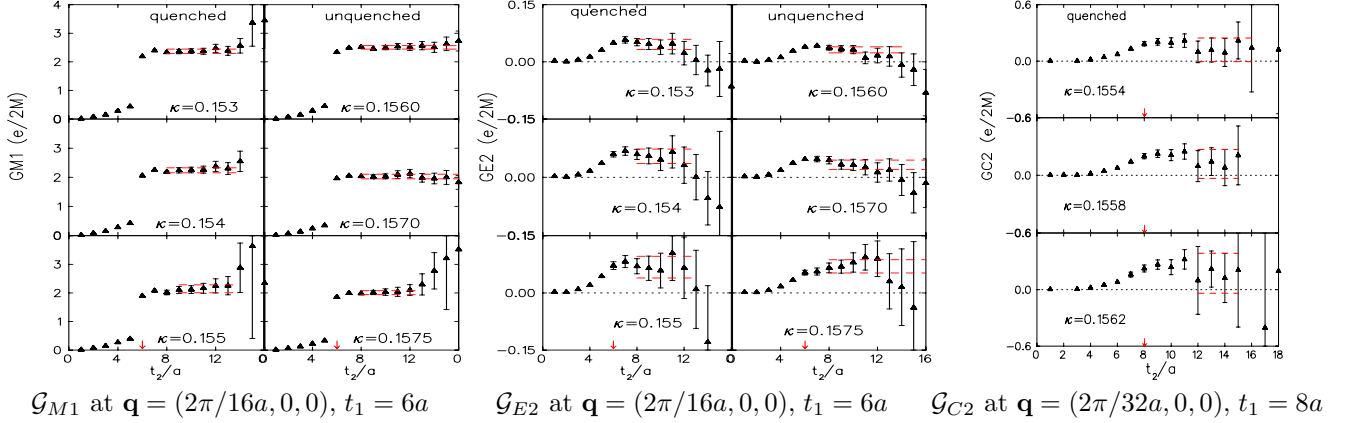


Figure 3. The dashed lines show the plateau fit range and bounds obtained by jackknife analysis.

ical form $g_0(1 + bQ^2) \exp(-cQ^2)F_D$ where $F_D = 1/(1 + Q^2/0.71)^2$ is the nucleon dipole form factor. Although lattice data are consistent with this form other parameterizations, such as simple exponential dependence, can not presently be excluded.

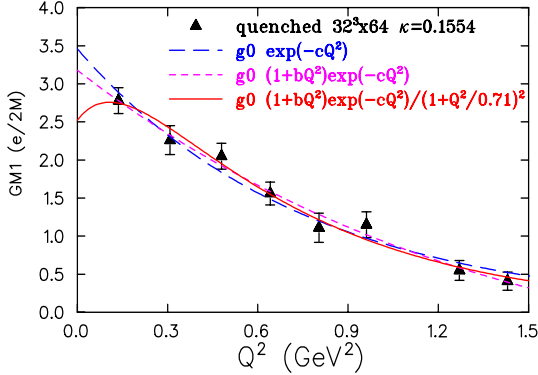


Figure 4. \mathcal{G}_{M1} versus Q^2 in the Δ rest frame.

Chiral extrapolation of the results is done linearly in the pion mass squared, since with the nucleon or the Δ carrying a finite momentum, chiral logs are expected to be suppressed. The values obtained are given in Table 2 and are in reasonable agreement with the experimental values $R_{EM} = -2.1 \pm 0.2 \pm 2.0$ at $Q^2 = 0.126 \text{ GeV}^2$ and $R_{EM} = -1.6 \pm 0.4 \pm 0.4$ at $Q^2 = 0.52 \text{ GeV}^2$.

4. Conclusions

1) The ratio R_{EM} has been computed for the first time with enough accuracy to exclude a zero

Table 2

$Q^2 \text{ GeV}^2$	$\mathcal{G}_{M1} (e/2m_N)$	$\mathcal{G}_{E2} (e/2m_N)$	$R_{EM} \%$
Quenched QCD			
0.64	1.70(6)	0.103(19)	-5.1(1.1)
0.13	2.53(6)	0.103(12)	-4.5(1.4)
Unquenched QCD			
0.53	1.30(4)	0.052(31)	-2.9(1.5)

value. In the kinematical regime explored by experiments we obtain values which are in agreement with recent measurements. 2) Large statistical and systematic errors prevent an accurate determination of the Coulomb quadrupole form factor. Although a zero value cannot be excluded, our results support a negative value of the ratio R_{SM} in agreement with experiment. 3) The detailed Q^2 dependence of the magnetic dipole transition can be evaluated with $\sim 10\%$ accuracy in the regime explored by JLab. 4) For pions in the range of 800-500 MeV no unquenching effects can be established for R_{EM} within our statistics.

REFERENCES

1. C. Alexandrou, Ph. de Forcrand, and A. Tsapalis, Phys. Rev. D **66** 094503 (2002); Nucl. Phys. B (Proc. Suppl.) **119** (2003) 422; hep-lat/0307009; this volume.
2. D. B. Leinweber, T. Draper, and R. M. Woloshyn, Phys. Rev. D **48**, (1993) 2230.
3. C. Alexandrou *et al.*, Nucl. Phys. B (Proc. Suppl.) **119** (2003) 413; hep-lat/0307018.
4. C.Mertz *et al.*, Phys. Rev. Lett. **86** (2001) 2963. K. Joo *et al.*, Phys. Rev. Lett. **88** (2002) 122001.
5. N. Eicker *et al.* [SESAM Collaboration], Phys. Rev. D **59** (1999) 014509.